한국광물학회지 제 15 권 제 2 호 (2002)
J. Miner. Soc. Korea, 15, 122-131 (2002)

Intergrowth and Interlayering of Muscovite, Chlorite, and Biotite in a Garnet Zone Metamorphic Rock of the Ogcheon Belt, South Korea

옥천대의 석류석대 변성암에서 산출되는 백운모, 녹니석 및 흑운모의 Intergrowth와 Interlayering

Yeong Boo Lee (이영부) · Jung Hoo Lee (이정후)* · Chang Whan Oh (오창환)

(Department of Earth and Environmental Sciences, Chonbuk National University, Chonju 561-756 Republic of Korea
(전북대학교 지구환경과학과)

ABSTRACT : Muscovite, chlorite and biotite in metapelites of the Ogcheon Metamorphic Belt are studied using electron probe microanalysis (EPMA), backscattered electron images (BEI) of scanning electron microscopy (SEM) and lattice fringe images of transmission electron microscopy (TEM). These minerals are observed to be intergrown under a polarized light microscope and are apparently interlayered below EPMA resolution; EPMA data often indicate mixtures of phyllosilicates such as muscovite/chlorite (M/C), biotite/chlorite (B/C), muscovite/pyrophyllite/chlorite (M/P/C), biotite/pyrophyllite/chlorite (B/P/C) or biotite/muscovite/chlorite (B/M/C). BEI observations show that the three minerals (muscovite, chlorite and biotite) are mixed at various scales in a grain through the garnet zone, and the interlayering of the three minerals are observed from TEM lattice fringe images and selected area electron diffraction patterns. The result of TEM observations reveals that 7-Å layers (serpentine, precursor of chlorite) are interlayered within 10-Å layers (muscovite) at 100~200 Å scale as well as M/C in the chlorite zone. The 7-Å layers become smaller in size and less frequent in the biotite zone, and 10-Å layers are interlayered with chlorite (14 Å) at an individual layer scale. The 7-Å layers are no longer observed in the garnet zone, and 10-Å layers (biotite) are interlayered with chlorite (B/C) at 50~100 Å scale. Relatively large scale (1000~2000 Å) of intergrowth is also frequently observed from the garnet zone samples. However, rocks from all three metamorphic zones show interlayering of a few units of 7-, 10- and 14-Å layers with each other at TEM observations. The result of this study implies that metamorphic minerals such as muscovite, chlorite and biotite form through disequilibrum mineral reactions resulting in inhomogenious phases.

Key words : muscovite, chlorite, biotite, Ogcheon Metamorphic Belt, intergrowth, interlayer, electron probe microanalysis, backscattered electron image, transmission electron microscopy

요약 : 옥천대 변성 이질암에 분포하는 백운모, 녹니석 및 흑운모는 각기 다른 크기에서 intergrowth와 interlayer 된 것을 전자현미분석(EPMA) 배면 산란 전자상(BEI) 관찰 및 투과 전자현미경(TEM)을 이용한 lattice fringe 상 관찰을 통한 연구에서 밝혔다. 이들 세 광물은 편광현미경 관찰에서도 intergrow된 것이 관찰되며 EPMA 분해능 이하의 크기에서는 interlayer된 것으로 보인다. 다시 말하면, EPMA 분석 자료는

*교신저자: jhlee@moak.chonbuk.ac.kr

흔히 백운모/녹니석(M/C), 흑운모/녹니석(B/C), 백운모/파이로필라이트/녹니석(M/Py/C), 흑운모/파이로필라이트/녹니석(B/Py/C) 또는 흑운모/백운모/녹니석(B/M/C)과 같이 두 개 이상의 phyllosilicate 광물의 혼합형태로 나타난다. BEI 관찰에서는 세 광물(백운모, 녹니석 및 흑운모)이 하나의 입자 안에서 다양한 크기로 섞여 있는 것으로 나타나며, TEM lattice fringe 상 관찰과 제한 시야 전자 회절상 관찰에 의하면 이들 세 광물 사이의 interlayering은 석류석대 변성암에서까지 관찰된다. TEM 관찰 결과 녹니석대 변성암에서는 M/C와 함께 7-Å layer(사문석, 녹니석의 전신)가 10-Å layer(백운모) 내에 100～200 Å 크기로 interlayer된 것이 밝혀졌다. 흑운모대 변성암으로 가면 7-Å layer는 크기와 발견 횟수가 감소하고 10-Å layer는 녹니석(14 Å)과 개별 layer 수준에서 interlayer된다. 석류석대 변성암에서는 7-Å layer는 더 이상 관찰되지 않으며 10-Å layer(흑운모)가 녹니석과 50～100 Å 크기로 interlayer된다(BEI, TEM). 석류석대 변성암에서는 비교적 큰 크기(1000～2000 Å)의 intergrowth가 흔히 관찰된다. 그러나 세 개의 변성대 암석은 모두 TEM 관찰에서 7-, 10-, 또는 14-Å layer들이 몇 개의 layer 단위에서 서로 interlayer된 것을 보여준다. 이와 같은 결과는 백운모, 녹니석 및 흑운모와 같은 변성 광물들이 비평형 광물 반응으로 만들어졌으며 그 결과 불균질한 광물로 되었다는 것을 암시한다.

주요어 : 백운모, 녹니석, 흑운모, 옥천 변성대, Intergrowth, Interlayer, 전자현미분석, 후방 산란 전자상, 투과 전자 현미경 관찰

Introduction

Sedimentary rocks go through diagenesis and metamorphism with the increase of temperature and pressure. Clay minerals in shale show changes in mineral composition with the evolution of diagenesis and metamorphism. Muscovite (or illite) and chlorite are the common minerals in the late stage of diagenesis and the early stage of metamorphism (chlorite zone). Biotite forms from the reaction of chlorite (biotite zone) and other metamorphic minerals (garnet, staurolite, kyanite and sillimanite) also form in the later stages of metamorphism. In the reactions of diagenesis and low-temperature metamorphism, muscovite and chlorite are generally formed, and the interlayering of smectite/illite (S/I), illite/chlorite (I/C), illite/serpentine (I/Sp) and muscovite/chlorite (M/C) are commonly observed (Lee *et al.*, 1984, 1985; Ahn and Peacor, 1986), which indicate disequilibrium reactions. These interlayered phases are known to evolve into homogeneous minerals with the increase of metamorphism or with the increase of temperature and pressure.

In a study of metapelites from the Ogcheon Metamorphic Belt (Fig. 1), a higher grade metamorphic rock, which is supposed to have homogeneous mineral grains, also show intergrowth between biotite, chlorite and muscovite in an observation of polarized light microscopy (PLM)(Fig. 2). Electron Probe microanalysis (EPMA) data and backscattered electron images (BEI) of muscovite, chlorite and biotite also show evidences of such intergrowth (Tables 1-4; Figs. 3, 4 and 5). This may indicate that mineral reactions in the higher grade metamorphism still occur under disequilibrium conditions resulting in heterogeneous mineral phases.

Experimental

The samples in this study are from chlorite, biotite and garnet zones of the Ogcheon Metamorphic Belt (Oh *et al.*, 1995a and b) (Fig. 1). Metapelite samples of the chlorite, biotite and garnet zones are cut perpendicular to the cleavage (foliation) of the metamorphic rock and thin sections are prepared. The PLM observations were carried out the same thin sections, and EPMA and BEI studies were performed using JEOL JXA-8600 Superprobe (EPMA) at a condition of 15 kV, 60 μA filament current and 2.0 nA PCD sample current. TEM observations were carried out on ion-thinned specimens that were taken from the same thin sections, using Philips CM-20 at 200 kV. EPMA analyses were focused on a grain that appear to have fine scale intergrowth of more than two phyllosilicate minerals from the

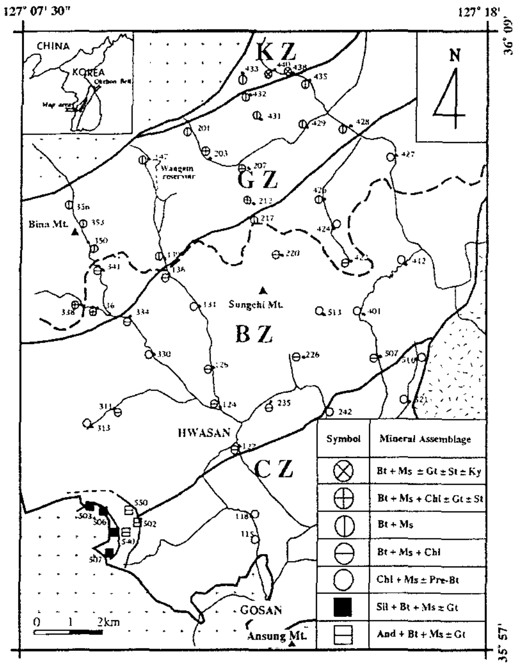

Fig. 1. The metamorphic map of the study area in the Ogcheon Metamorphic Belt. Symbols on the map indicate the mineral assemblages at the sample location (Bt, biotite; Ms, muscovite; Gt, garnet; St, staurolite; Ky, kyanite; Chl, chlorite; Pre-Bt, pre-stage biotite; Sil, sillimanite and And, andalusite). The numbers represent the sample numbers. CZ, chlorite zone; BZ, biotite zone; GZ, garnet zone and KZ, Kyanite zone. The areas marked with crosses and random hatchers are Jurassic granite and Cretaceous granite, respectively (see Oh *et al.*, 1995a for detail).

Fig. 2. A Polarized light photomicrograph (cross nicol) of a garnet zone metapelite from the Ogcheon Metamorphic Belt. The micas are oriented parallel to the cleavage running from the upper left to the lower right. The sample is cut perpendicular to the cleavage (foliation). The sample is composed of biotite (B; medium gray), muscovite (M; light gray), chlorite (C; dark gray) and quartz (Q; black, gray to white). The intergrowths between muscovite and biotite (M/B), chlorite and muscovite (C/M) and chlorite, muscovite and biotite (C/M/B) are commonly observed.

BEI observations and compared with the analyses of seemingly homogeneous single phases.

Results

Polarized Light Microscopy

Muscovite, chlorite and biotite show strong preferred orientation parallel to the cleavage of the metamorphic rock (Fig. 2). Most of the three minerals seems to be intergrown with each other in various scales. Intergrowth of muscovite/chlorite (M/C), biotite/muscovite (B/M) and biotite/muscovite/chlorite (B/M/C) are commonly observed.

Backscattered Electron Images

Muscovite, chlorite and biotite show different contrasts in BEI, and they can be identified from such differences. Biotite with relatively heavier elements shows the brightest contrast among the three, and muscovite with lighter elements shows the darkest contrast. Chlorite shows an intermediate contrast (Figs. 3, 4 and 5). Biotite in a biotite zone metamorphic rock shows fine scale intergrowths with chlorite (biotite/chlorite or B/C) along the cleavage. Some of these intergrowths appear to be muscovite (B/M) with darker contrasts within the biotite grain. Muscovite and chlorite also show intergrowth of M/C (muscovite matrix with chlorite interlayered) and C/M (chlorite matrix with muscovite interlayered), respectively (Fig. 4). The garnet zone sample also shows intergrowth of B/C, B/M and B/M/C as well as

Table 1. Muscovite in Manhang Formation

Sample#	M10											
Analysis#	12	13	29	30	15	26	11	19	20	23	24	25
Oxide wt.%												
SiO_2	44.91	44.57	44.36	44.05	44.20	44.22	48.75	43.92	44.55	44.88	46.27	59.61
Al_2O_3	35.43	35.17	34.83	34.98	34.35	33.52	35.28	35.39	35.12	34.52	34.84	29.79
TiO_2	0.00	0.00	0.02	0.00	0.11	0.31	0.00	0.07	0.00	0.00	0.01	0.00
FeO	1.54	1.53	1.71	1.56	2.69	1.71	1.79	1.71	3.21	1.36	1.48	0.57
MgO	0.34	0.34	0.37	0.29	0.47	0.93	0.35	0.24	0.33	0.34	0.29	0.09
MnO	0.01	0.01	0.00	0.00	0.01	0.00	0.00	0.00	0.07	0.00	0.03	0.02
Cr_2O_3	0.01	0.01	0.00	0.05	0.03	0.00	0.00	0.01	0.00	0.02	0.01	0.00
CaO	0.04	0.03	0.07	0.06	0.01	0.04	0.00	0.04	0.05	0.17	0.03	0.14
Na_2O	0.43	0.37	0.46	0.37	0.63	0.40	0.25	0.26	0.31	0.35	0.36	0.09
K_2O	10.28	10.18	10.03	10.37	9.85	10.22	7.01	6.96	8.62	8.59	9.51	1.01
Total	92.98	92.20	91.84	91.73	92.37	91.35	93.44	88.59	92.24	90.22	92.82	91.31
	Atomic proportion based on $O_{20}(OH)_4$											
Si	6.13	6.13	6.13	6.10	6.11	6.16	6.44	6.15	6.12	6.23	6.27	7.56
Al	5.69	5.70	5.67	5.71	5.60	5.50	5.49	5.84	5.68	5.65	5.57	4.46
Ti	0.00	0.00	0.00	0.00	0.01	0.03	0.00	0.01	0.00	0.00	0.00	0.00
Fe^{2+}	0.18	0.18	0.20	0.18	0.31	0.20	0.20	0.20	0.37	0.16	0.17	0.06
Mg	0.07	0.07	0.08	0.06	0.10	0.19	0.07	0.05	0.07	0.07	0.06	0.02
Mn	0.01	0.00	0.00	0.00	0.00	0.00	0.00	0.00	0.01	0.00	0.00	0.00
Cr	0.00	0.00	0.00	0.01	0.00	0.00	0.00	0.00	0.00	0.00	0.00	0.00
Ca	0.01	0.00	0.01	0.01	0.00	0.01	0.00	0.01	0.01	0.03	0.00	0.02
Na	0.11	0.10	0.12	0.10	0.17	0.11	0.07	0.07	0.08	0.10	0.09	0.02
K	1.79	1.79	1.77	1.83	1.74	1.82	1.18	1.24	1.51	1.52	1.64	0.16
Int. Tot.	1.91	1.89	1.90	1.94	1.91	1.93	1.25	1.32	1.60	1.64	1.74	0.20
Oct. Tot.	4.07	4.08	4.08	4.06	4.13	4.09	4.19	4.25	4.24	4.11	4.07	4.10
	Single Phase						Mixed Phase					

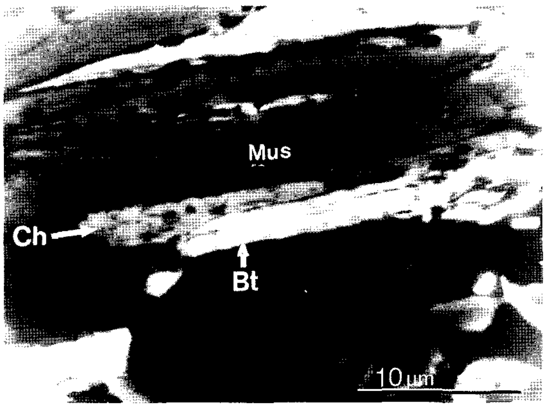

Fig. 3. A backscattered electron image (BEI) of a chlorite zone sample from the Ogcheon Metamorphic Belt. Muscovite (Mus) is the most abundant and shows dark contrast among the three minerals. Chlorite (Chl) is also abundant and shows intermediate contrast between muscovite and biotite. Biotite (Bt) is rare in the chlorite zone sample and show bright contrast.

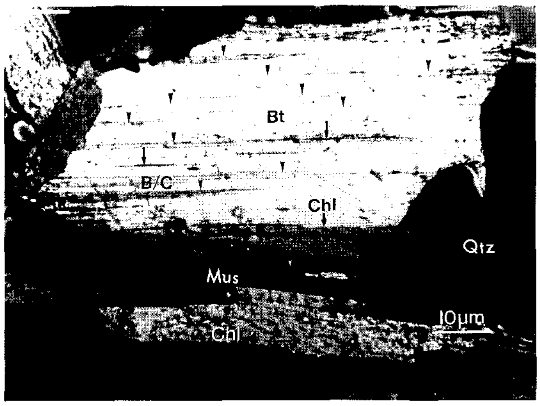

Fig. 4. A backscattered electron image (BEI) of a biotite zone sample from the Ogcheon Metamorphic Belt. Biotite (Bt) is the predominant among the three minerals and show fine scale intergrowth of chlorite (B/C, indicated as black arrow heads) and muscovite (B/M, black arrows). Chlorite (Chl) and muscovite (Mus) are apparently intergrown with biotite at a scale of 5 ~ 10 μm within a gran. Chlorite and muscovite seem to have areas of C/M or M/C intergrowth (white arrow heads).

M/C (Fig. 5).

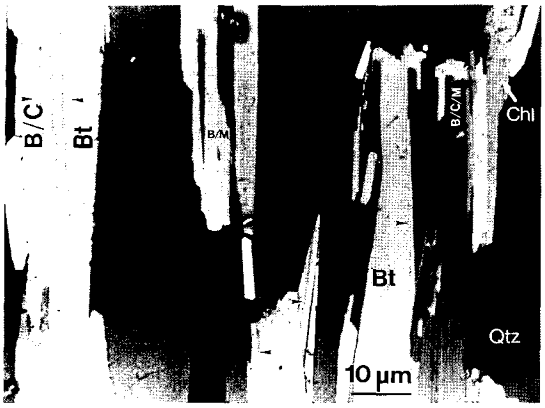

Fig. 5. A backscattered electron image (BEI) of a garnet zone sample from the Ogcheon Metamorphic Belt. Chlorite (Chl) is less abundant compared with muscovite (Mus) and biotite (Bt). Biotite show various scales of intergrowth with chlorite (B/C and arrow heads) near the left side margin and intergrowth with muscovite (B/M) at the upper middle. Biotite, muscovite and chlorite seem to be intergrown as a single grain on the whole. Near the upper right corner, the three minerals appear to be intergrown (B/C/M) at a fine scale. Quartz (Qtz) appears as black areas.

Electron Probe Microanalyses

Analyses of muscovite, chlorite and biotite were performed in the areas which show interlayering (or intergrowth) of other phases (mixed phase in Tables 1-4) and compared with the areas of no interlayering (single phase). The compositions of mixed phase show significant differences especially in total interlayer cations and total octahedral cations (Tables 1-4). This represents the mixing of different mineral compositions in the mixed phases. The composition and the content of the component minerals can be estimated. The interlayering of three minerals such as M/Py/C(muscovite/pyrophyllite/chlorite), B/M/C and B/Py/C as well as M/C, M/Py, B/M and B/C are confirmed from the calculation (Kim, 1992; Lee, 1993; Baek, 1994)

Muscovite

Analyses of mixed phase muscovite show lower values (less than 2.0) in interlayer cations (sum of K, Na, and Ca) and excess values

Table 2. Minerals in chlorite zone

	Muscovite						Chlorite					
Sample#	1501						1501-2					
Analysis#	5	6	7	25	26	32	11	40	41	42	40	61
Oxide wt.%												
SiO_2	46.13	45.49	46.17	46.99	46.07	46.44	25.02	25.00	24.45	27.22	25.89	30.08
Al_2O_3	35.44	36.40	35.82	33.38	34.03	33.05	24.24	23.41	23.68	25.65	23.77	19.48
TiO_2	0.67	0.66	0.54	0.62	0.29	0.69	0.12	0.21	0.00	0.21	0.13	0.19
FeO	1.26	1.24	1.08	1.51	1.24	1.45	20.33	22.94	22.56	19.79	20.82	20.87
MgO	0.85	0.67	0.81	0.87	0.83	0.82	17.58	16.25	15.62	12.82	15.34	13.53
MnO	0.15	0.00	0.03	0.14	0.16	0.00	0.06	0.07	0.31	0.31	0.22	0.06
Cr_2O_3	0.05	0.00	0.22	0.17	0.08	0.09	0.00	0.00	0.00	0.00	0.12	0.07
CaO	0.00	0.09	0.00	0.06	0.08	0.04	0.07	0.12	0.08	0.00	0.00	0.12
Na_2O	0.55	0.63	0.73	0.00	0.33	0.00	0.19	0.25	0.28	0.44	0.32	0.47
K_2O	9.73	9.53	9.81	8.48	8.77	8.62	0.16	0.03	0.01	2.21	1.56	1.79
Total	94.83	94.71	95.10	92.21	91.79	91.19	87.77	88.28	86.99	88.65	88.17	86.65
	Atomic proportion based on $O_{20}(OH)_4$						Atomic proportion based on $O_{20}(OH)_{16}$					
Si	6.14	6.06	6.13	6.37	6.29	6.37	5.13	5.16	5.13	5.85	5.64	6.27
Al	5.56	5.72	5.61	5.33	5.48	5.34	5.85	5.70	5.85	6.11	5.70	4.79
Ti	0.07	0.07	0.05	0.06	0.03	0.07	0.02	0.03	0.00	0.03	0.02	0.03
Fe^{2+}	0.14	0.14	0.12	0.17	0.14	0.17	3.48	3.96	3.96	3.10	3.54	3.64
Mg	0.17	0.13	0.16	0.18	0.17	0.17	5.37	5.00	4.88	3.58	4.10	4.20
Mn	0.02	0.00	0.00	0.02	0.02	0.00	0.01	0.01	0.06	0.05	0.04	0.01
Cr	0.01	0.00	0.01	0.02	0.00	0.01	0.00	0.00	0.00	0.00	0.02	0.01
Ca	0.00	0.01	0.00	0.01	0.01	0.01	0.01	0.03	0.02	0.00	0.00	0.03
Na	0.14	0.16	0.19	0.00	0.09	0.00	0.08	0.10	0.11	0.16	0.13	0.19
K	1.65	1.62	1.66	1.47	1.53	1.51	0.04	0.01	0.00	0.53	0.43	0.48
Int. Tot.	1.80	1.78	1.85	1.48	1.63	1.51	0.13	0.13	0.13	0.69	0.56	0.69
Oct. Tot.	4.12	4.11	4.09	4.15	4.12	4.13	11.86	11.88	11.87	10.72	11.05	10.95
	Single Phase			Mixed Phase			Single Phase			Mixed Phase		

Table 3. Minerals in biotite zone

	Muscovite						Biotite					
Sample#	5252-6						51107-2					
Analysis#	11	12	71	162	169	207	155	190	194	19	22	58
Oxide wt.%												
P_2O_5	0.01	0.00	0.01	0.04	0.01	0.00	0.00	0.00	0.00	0.03	0.00	0.00
SiO_2	45.03	44.59	43.64	40.43	40.53	43.16	33.86	33.96	34.76	31.61	31.91	33.03
Al_2O_3	35.63	35.59	34.00	30.64	29.61	33.16	17.51	17.78	17.15	17.61	18.46	17.91
TiO_2	0.32	0.31	0.35	0.37	0.31	0.31	1.68	1.80	1.66	1.29	1.16	1.63
FeO	0.80	0.70	1.20	6.54	6.04	3.15	19.90	20.58	20.32	19.41	19.17	19.47
MgO	0.44	0.42	0.70	3.08	3.86	1.74	9.81	9.86	10.22	13.41	13.30	12.02
MnO	0.00	0.01	0.00	0.15	0.16	0.09	0.25	0.15	0.13	0.09	0.02	0.21
CaO	0.00	0.00	0.00	0.14	0.02	0.06	0.01	0.00	0.00	0.05	0.03	0.00
Na_2O	1.88	1.74	0.88	0.22	0.20	0.50	0.10	0.09	0.04	0.08	0.00	0.05
K_2O	8.23	8.56	9.76	7.71	8.00	9.02	8.81	8.90	8.83	5.78	5.42	7.03
Total	92.33	91.91	90.54	89.31	88.71	91.18	91.93	93.12	93.11	89.36	89.47	91.34
	Atomic proportion based on $O_{20}(OH)_4$											
P	0.00	0.00	0.00	0.01	0.00	0.00	0.00	0.00	0.00	0.00	0.00	0.00
Si	6.12	6.10	6.11	5.89	5.94	6.05	5.38	5.34	5.45	5.10	5.10	5.23
Al	5.71	5.74	5.61	5.26	5.11	5.48	3.28	3.30	3.17	3.35	3.48	3.34
Ti	0.03	0.03	0.04	0.04	0.03	0.03	0.20	0.21	0.20	0.16	0.14	0.19
Fe^{2+}	0.09	0.08	0.14	0.80	0.74	0.37	2.65	2.71	2.66	2.62	2.56	2.58
Mg	0.09	0.09	0.15	0.67	0.84	0.36	2.32	2.31	2.39	3.22	3.17	2.83
Mn	0.00	0.00	0.00	0.02	0.02	0.01	0.03	0.02	0.02	0.01	0.00	0.03
Ca	0.00	0.00	0.00	0.02	0.00	0.01	0.00	0.00	0.00	0.01	0.01	0.00
Na	0.50	0.46	0.24	0.06	0.06	0.14	0.03	0.03	0.01	0.03	0.00	0.01
K	1.43	1.49	1.74	1.43	1.50	1.61	1.79	1.79	1.77	1.19	1.11	1.42
Int. Tot.	1.92	1.95	1.98	1.52	1.56	1.76	1.82	1.81	1.78	1.22	1.11	1.43
Oct. Tot.	4.04	4.03	4.05	4.67	4.69	4.30	5.87	5.89	5.88	6.45	6.46	6.20
	Single Phase			Mixed Phase			Single Phase			Mixed Phase		

Table 3. Continued

	Chlorite											
Sample#	51107-2						51107-2					
Analysis#	110	119	120	121	130	136	34	46	62	111	145	150
Oxide wt.%												
P_2O_5	0.04	0.00	0.01	0.06	0.09	0.00	0.00	0.00	0.00	0.00	0.00	0.00
SiO_2	23.89	23.81	23.85	23.88	24.16	23.83	28.16	26.77	27.61	25.74	28.55	26.28
Al_2O_3	21.77	22.19	22.22	22.21	21.77	22.64	19.01	18.79	18.67	20.43	18.18	17.38
TiO_2	0.12	0.06	0.07	0.11	0.12	0.09	0.35	0.23	0.38	0.21	0.52	0.22
FeO	23.67	24.57	24.30	24.94	24.32	25.99	22.72	21.86	20.99	23.62	26.18	27.70
MgO	16.13	15.14	15.80	15.60	14.57	14.19	17.14	17.67	16.64	15.53	12.68	13.19
MnO	0.15	0.14	0.16	0.25	0.05	0.35	0.14	0.18	0.14	0.12	0.30	0.22
CaO	0.04	0.00	0.02	0.02	0.01	0.03	0.01	0.00	0.01	0.02	0.10	0.08
Na_2O	0.07	0.00	0.00	0.01	0.00	0.00	0.00	0.00	0.00	0.00	0.04	0.00
K_2O	0.06	0.00	0.00	0.02	0.10	0.01	1.23	0.58	1.25	1.03	1.88	0.94
Total	89.04	88.54	86.33	85.60	89.01	89.01	85.60	86.24	85.78	85.72	84.98	83.56
	Atomic proportion based on $O_{20}(OH)_{16}$											
P	0.00	0.00	0.00	0.01	0.02	0.00	0.00	0.00	0.00	0.00	0.00	0.00
Si	5.12	5.12	5.09	5.08	5.23	5.09	5.80	5.67	5.85	5.48	6.04	5.78
Al	5.50	5.63	5.59	5.57	5.55	5.70	4.61	4.69	4.66	5.12	4.53	4.51
Ti	0.02	0.01	0.01	0.02	0.02	0.01	0.05	0.04	0.06	0.03	0.08	0.04
Fe^{2+}	4.24	4.42	4.34	4.44	4.40	4.64	3.91	3.87	3.72	4.20	4.63	5.09
Mg	5.15	4.85	5.03	4.94	4.70	4.52	5.26	5.58	5.26	4.92	4.00	4.32
Mn	0.03	0.03	0.03	0.05	0.01	0.06	0.03	0.03	0.03	0.02	0.05	0.04
Ca	0.01	0.00	0.00	0.01	0.00	0.01	0.00	0.00	0.00	0.00	0.02	0.02
Na	0.03	0.00	0.00	0.00	0.00	0.00	0.00	0.00	0.00	0.00	0.02	0.00
K	0.02	0.00	0.00	0.01	0.03	0.00	0.32	0.16	0.34	0.28	0.51	0.26
Int. Tot.	0.06	0.00	0.00	0.01	0.03	0.01	0.33	0.16	0.34	0.28	0.54	0.28
Oct. Tot.	12.06	12.06	12.09	12.09	11.92	12.04	11.67	11.87	11.58	11.78	11.33	11.78
	Single Phase						Mixed Phase					

(greater than 4.0) in octahedral cations (mainly the sum of Al^{VI}, Fe and Mg) compared with single phase muscovite (Tables 1-4) showing an ideal composition of $K_2Al_4(Si_6Al_2)O_{20}(OH)_4$. The deviation from an ideal value results from the mixing with phases of lower interlayer cations (chlorite or pyrophyllite) and higher octahedral cations (chlorite or biotite). The major mixed (or interlayered) phase with muscovite is chlorite (M/C). However, pyrophyllite or biotite interlayered with muscovite (M/Py, M/B) are sometimes observed (Figs. 4, 5 and 10). The interlayering of M/Py/C is also confirmed by the estimation of component minerals using ideal compositions of muscovite and pyrophyllite and the differences in the total interlayer and octahedral cations (Kim, 1992; Lee, 1993; Baek, 1994).

Chlorite

Analyses of mixed phase chlorite show considerable amount of interlayer cations (K, Na and Ca) and significantly low values (less than 12.0) of total octahedral cations (Tables 2, 3 and 4). Comparison of our data with ideal chlorite composition (no interlayer and 12 octahedral cations), implies the mixing of other minerals with interlayer cations (muscovite or biotite) and less octahedral cations (muscovite, biotite or pyrophyllite). The calculation of the component minerals mixed with chlorite revealed the interlayering of M/Py/C, B/M/C and B/Py/C as well as M/C and B/C (Kim, 1992; Lee, 1993; Baek, 1994).

Biotite

Analyses of mixed phase biotite show considerably lower values in total interlayer cations (less than 2.0) and significant deviation in the number of total octahedral cations (much lower or greater than 6.0). Since an ideal biotite contains 2.0 interlayer cations (K) and 6.0 octahedral cations, the lower values in interlayer cation imply the interlayering of chlorite or pyrophyllite; lower octahedral cations, muscovite or pyrophyllite and higher octahedral cations,

Table 4. Minerals in garnet zone

	Muscovite						Biotite					
Sample#	1203-2						1203-2					
Analysis#	34	22	43	15	9	11	8	14	45	24	15	2
Oxide wt.%												
SiO_2	45.56	45.39	45.29	45.49	43.11	45.50	39.58	35.75	33.81	36.59	33.44	33.74
Al_2O_3	36.03	36.02	33.89	36.40	34.63	35.57	27.19	20.01	18.03	30.82	20.09	20.01
TiO_2	0.42	0.55	0.74	0.66	0.53	0.42	1.36	1.54	1.51	0.44	1.03	1.32
FeO	1.24	1.07	0.30	1.24	1.88	1.25	12.10	16.35	20.39	6.64	16.86	17.10
MgO	0.67	0.38	0.92	0.67	0.73	0.76	7.64	12.14	9.19	4.54	12.96	12.86
MnO	0.10	0.00	0.24	0.00	0.00	0.00	0.15	0.47	0.28	0.00	0.22	0.20
Cr_2O_3	0.00	0.15	0.00	0.00	0.03	0.07	0.13	0.00	0.00	0.07	0.07	0.06
CaO	0.17	0.00	0.00	0.09	0.00	0.00	0.00	0.00	0.00	0.02	0.00	0.00
Na_2O	0.99	0.68	1.02	0.63	0.66	0.71	0.49	0.28	0.27	0.25	0.38	0.29
K_2O	9.60	9.66	8.73	9.53	8.39	9.26	9.56	9.16	9.19	4.79	7.19	7.47
Total	94.78	93.90	91.13	94.71	89.96	93.53	98.10	95.70	92.67	84.17	92.23	93.04
Atomic proportion based on $O_{20}(OH)_4$												
Si	6.08	6.10	6.24	6.06	6.04	6.13	5.53	5.33	5.35	5.59	5.16	5.17
Al	5.67	5.71	5.51	5.72	5.72	5.65	4.47	3.52	3.36	5.55	3.65	3.61
Ti	0.04	0.06	0.08	0.07	0.06	0.04	0.14	0.17	0.18	0.05	0.12	0.15
Fe^{2+}	0.14	0.12	0.03	0.14	0.22	0.14	1.41	2.04	2.70	0.85	2.18	2.19
Mg	0.13	0.08	0.11	0.13	0.15	0.15	1.59	2.70	2.17	1.03	2.98	2.94
Mn	0.01	0.00	0.05	0.00	0.00	0.00	0.02	0.06	0.03	0.00	0.03	0.03
Cr	0.00	0.02	0.00	0.00	0.00	0.01	0.01	0.00	0.00	0.01	0.01	0.01
Ca	0.03	0.00	0.00	0.01	0.00	0.00	0.00	0.00	0.00	0.00	0.00	0.00
Na	0.26	0.18	0.27	0.16	0.18	0.18	0.13	0.08	0.08	0.07	0.11	0.09
K	1.63	1.66	1.54	1.62	1.50	1.59	1.70	1.74	1.86	0.93	1.42	1.46
Int. Tot.	1.89	1.83	1.81	1.78	1.68	1.78	1.83	1.82	1.94	1.01	1.53	1.55
Oct. Tot.	4.09	4.07	4.01	4.11	4.20	4.12	5.19	5.88	5.80	5.08	6.16	6.12
	Single Phase			Mixed Phase			Single Phase			Mixed Phase		

Table 4. Continued

	Chlorite											
Sample#	1338-2						1203					
Analysis#	33	56	61	66	67	84	28	23	49	48	78	43
Oxide wt.%												
SiO_2	23.81	24.52	24.41	24.48	24.67	24.65	25.89	23.87	27.51	26.25	24.66	25.26
Al_2O_3	23.04	23.76	23.53	23.70	24.06	23.82	23.77	23.18	20.13	19.65	24.40	23.81
TiO_2	0.07	0.02	0.03	0.08	0.00	0.00	0.13	0.00	0.25	0.00	0.04	0.15
FeO	23.43	23.86	23.92	22.26	19.39	18.63	20.82	19.80	25.53	26.07	20.97	22.38
MgO	13.92	13.66	13.62	14.90	16.50	16.16	16.83	16.18	13.98	13.39	14.95	16.25
MnO	0.12	0.14	0.15	0.10	0.21	0.19	0.22	0.22	0.00	0.36	0.04	0.33
Cr_2O_3	0.05	0.06	0.00	0.00	0.00	0.00	0.12	0.02	0.00	0.00	0.00	0.09
CaO	0.00	0.00	0.00	0.04	0.07	0.04	0.00	0.00	0.00	0.08	0.09	0.07
Na_2O	0.04	0.12	0.03	0.05	0.03	0.01	0.32	0.39	0.34	0.41	0.43	0.50
K_2O	0.06	0.08	0.08	0.10	0.05	0.06	0.94	0.30	0.81	0.14	0.03	0.18
Total	84.54	86.24	85.78	85.72	84.98	83.56	89.04	83.96	88.54	86.33	85.60	89.01
Atomic proportion based on $O_{20}(OH)_{16}$												
Si	5.17	5.27	5.22	5.19	5.19	5.25	5.26	5.13	5.75	5.66	5.20	5.17
Al	5.89	5.95	5.93	5.92	5.97	5.98	5.70	5.88	4.96	4.99	6.06	5.74
Ti	0.01	0.01	0.01	0.02	0.01	0.01	0.02	0.00	0.04	0.00	0.01	0.02
Fe^{2+}	4.25	4.24	4.28	3.95	3.41	3.43	3.54	3.56	4.46	4.70	3.70	3.83
Mg	4.50	4.33	4.34	4.71	5.18	5.13	5.10	5.19	4.35	4.30	4.70	4.96
Mn	0.02	0.03	0.03	0.02	0.04	0.03	0.04	0.04	0.00	0.07	0.01	0.06
Cr	0.01	0.01	0.00	0.00	0.00	0.00	0.02	0.00	0.00	0.00	0.00	0.01
Ca	0.00	0.00	0.00	0.01	0.02	0.01	0.00	0.00	0.00	0.02	0.02	0.02
Na	0.02	0.05	0.01	0.02	0.01	0.01	0.13	0.16	0.14	0.17	0.18	0.20
K	0.02	0.01	0.01	0.02	0.00	0.00	0.24	0.08	0.22	0.04	0.03	0.05
Int. Tot.	0.03	0.06	0.02	0.05	0.03	0.02	0.37	0.25	0.35	0.23	0.22	0.26
Oct. Tot.	11.86	11.83	11.80	11.80	11.80	11.84	11.67	11.80	11.56	11.72	11.66	11.79
	Single Phase						Mixed Phase					

chlorite. The interlayering of B/M/C and B/Py/C was confirmed by the chemical calculation as well as the observation of B/M, B/C and B/Py (Kim, 1992; Lee, 1993; Baek, 1994).

Transmission Electron Microscopy

Muscovite and chlorite are predominant phases in the chlorite zone metamorphic rock of the Ogcheon Belt and the sedimentary rock of the Chinan Group. These rocks show interlayering of chlorite (14 Å) within predominant (single phase) muscovite (10 Å) (Fig. 6) and of muscovite within single phase chlorite (Fig. 7) at the TEM observations. The interlayering occurs mainly in a scale of few layers thick and are randomly distributed causing the streaking in the SAED pattern. 7-Å layers (serpentine-like layers) are also interlayered with 10 and 14-Å layers (Fig. 6). Garnet zone metamorphic rocks consist mainly of biotite, muscovite and chlorite and also show interlayering of chlorite (14 Å) and mica (10 Å) at a scale of few layers to several hundreds of angstroms (Figs. 8

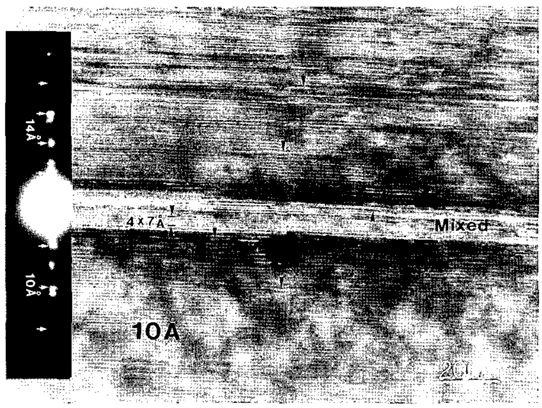

Fig. 6. A transmission electron photomicrograph of lattice fringes of muscovite (10 Å, 001 layers), chlorite (14 Å) and serpentine (7 Å) in the sample from chlorite zone metamorphic rock of the Ogcheon Belt. Muscovite show predominant 10-Å lattice fringes with some 14-Å (chlorite) fringes (indicated by arrow heads) and a small band of 7-Å (serpentine) layers. Along with the serpentine layers is a mixed area of 10-, 14- and 7-Å layers with lighter contrast. This light contrast area seems to be more easily damaged by the electron beam. The selected area electron diffraction (SAED) pattern on the inset show 10- and 14-Å periodicities of *00l* reflections from muscovite and chlorite.

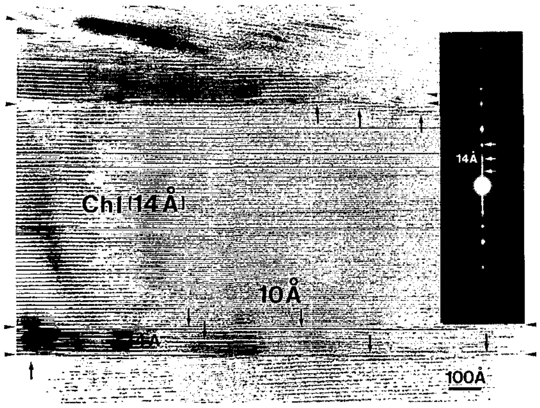

Fig. 7. A TEM lattice fringe image of a shale sample from the Cretaceous Chinan Group sedimentary rock. Chlorite (Chl) is the predominant phase in this grain and some 10-Å (muscovite) layers (indicated by arrows) are also present. Slight off angle boundaries (along the arrow heads marked on the both left and right margins) seem to be grain boundaries between two grains merging into one. Interlayering (or intergrowth) between chlorite and muscovite in this sedimentary rock is similar to that of chlorite zone metamorphic rock of the Ogcheon Belt. Chlorite shows 7-Å half fringes on the right hand side due to the decrease of the sample thickness. SAED pattern on the inset show streaking along *00l* reflections caused by mixed layering of 14- and 10-Å fringes.

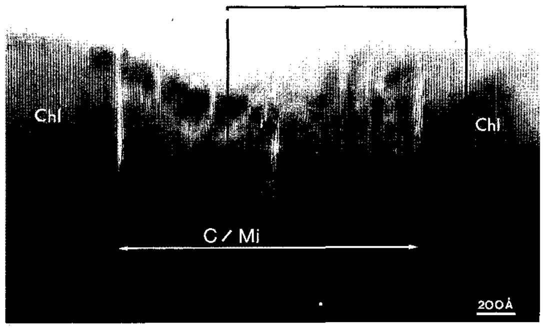

Fig. 8. A TEM lattice fringe image of the garnet zone metamorphic rock from the Ogcheon Belt. The chlorite (Chl) dominant grain has an area of interlayering between chlorite and mica (C/Mi). The mica layers have the 10-Å periodicity and it probably is either muscovite or biotite. The area within the rectangle is enlarged in Fig. 9.

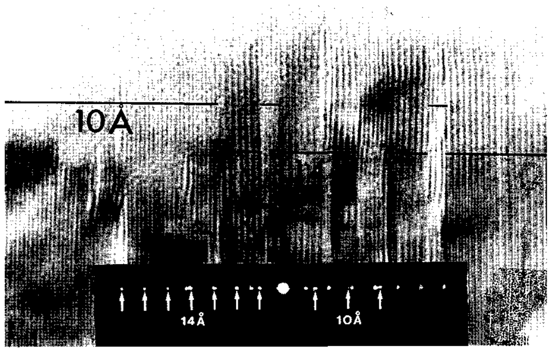

Fig. 9. An enlarged view of the marked area in Fig. 8. 10- and 14-Å layers are interlayered in a scale of 50~200 Å. The lattice fringes show electron beam damage mainly at the boundaries causing distortions of the layer. The SAED pattern on the inset shows sharp 10- and 14-Å periodicities.

and 9). Pyrophyllite (9.3 Å) is also observed to be interlayered with muscovite (10 Å) at a scale of 200~300 Å as well as at an individual layer scale in the Manhang Formation (Fig. 10).

Discussion and Conclusions

Shale from the Chinan Group (Kim, 1992) and the Manhang Formation (Lee, 1993) contains muscovite and chlorite, and the metapelites from the Ogcheon Belt contain muscovite, chlorite, and biotite as major phyllosilicates. These minerals are intergrown and interlayered at various scales from an individual layer level to few thousand angstroms as observed using PLM, BEI and TEM lattice fringe images. The interlayering (or intergrowth) causes the variation of chemical compositions in analyses of these minerals. Mixing of three minerals is common in low-grade metamorphic rocks. The interlayering seems to generate some deviation from an ideal composition even in the analysis of single phase minerals. Pyrophyllite is also

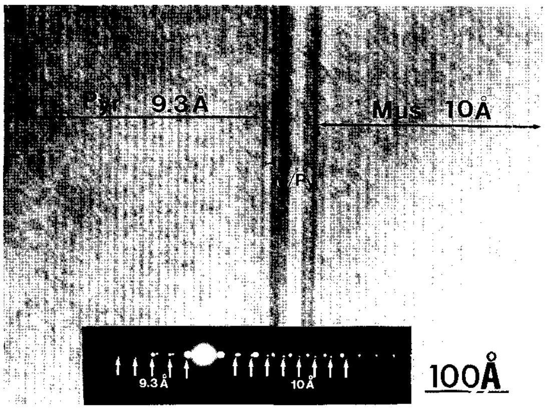

Fig. 10. A TEM lattice fringe image of muscovite (Mus) and pyrophyllite (Pyr) in a shale from the Carboniferous Manhang Formation. Pyrophyllite (d_{001}=9.3 Å) is intergrown with muscovite (d_{001}= 10 Å) at a scale of 200~300 Å (The full range of intergrowth is not shown here). The thickness of 10 layers of pyrophyllite (93 Å) is approximately the same as that of 9 layers of muscovite (90 Å). The SAED pattern on the inset also shows discrete *00l* reflections of muscovite and pyrophyllite with periodicities of 10 and 9.3 Å, respectively. The area between the two phases (between the two arrow heads) is transitional with the seemingly interlayered muscovite and pyrophyllite (M/Py).

involved in this interlayering (Jiang *et al.*, 1990), and serpentine plays a role as a precursor of chlorite. Interlayering between muscovite, chlorite and biotite, including pyrophyllite appears to be common not only in the sedimentary and low grade metamorphic rocks, but also in the higher grade metamorphic rocks implying that disequilibrium reactions are pervasive throughout the metamorphism.

References

Ahn, J.H. and Peacor D.R. (1986) Transmission and analytical electron microscopy of the smectite to illite transition. Clays and Clay Minerals, 34, 165-179.

Baek, J.H. (1994) A Mineralogical study of layer silicates in the metamorphic rocks form the southwestern part of the Ogcheon Metamorphic Belt (in Korean). M.S. Thesis, Chonbuk National University, 1994, 81p.

Jiang, W.T., Essene E.J., and Peacor D.R. (1990) Transmission electron microscopic study of coexisting pyrophyllite and muscovite: Direct evidence for the metastability of illite. Clays and Clay Minerals, 38, 225-240.

Kim, Y.H. (1992) A mineralogical study of clay minerals in the shale of the Chinan Basin (in Korean). M.S. Thesis, Chonbuk National University, 1992, 72p.

Lee, J.H., Peacor, D.R. Lewies D.D., and Wintsh R.P. (1984) Chlorite-illite/muscovite interlayered and interstratified crystals: A TEM/STEM study. Contributions to Mineralogy and Petrology, 88, 372-385.

Lee, J.H., Ahn J.H., and Peacor D.R. (1985) Textures in layered silicates: Progressive changes through diagenesis and low temperature metamorphism. Journal of Sedimentary Petrology, 55, 532-540.

Lee, Y.B. (1993) Mineralogical studies of phyllosilicates on the diagenesis and metamorphism of the Jigunsan and Manhang Formation: EPMA/ TEM Study (in Korean). M.S. Thesis, Chonbuk National University, 1993, 58p.

Oh, C.W., Kim S.T., and Lee J.H. (1995a) The metamorphic evolution in the southwestern part of the Okcheon Metamorphic Belt. Journal of Geological Society of Korea, 31, 21-31.

Oh, C.W., Kim S.T., and Lee J.H. (1995b) The P-T condition and timing of the main metamorphism in the southwestern part of the Okcheon Metamorphic Belt. Journal of the Geological Society of Korea, 31, 343-361.

2002년 5월 21일 원고접수, 2002년 6월 8일 게재승인.